Critical Marangoni numbers and their effect on the dopant distribution in silicon fibers

L. Braescu, and T. F. George

***Abstract*—**The dependence of the Marangoni flow and impurity distribution on the vertical temperature gradient is analyzed in the framework of a stationary model including the incompressible Navier-Stokes equation in the Boussinesq approximation and the convection-conduction, and conservative convection-diffusion equations. The computations are carried out in a 2D axisymmetric model by the finite-element numerical technique, for aluminum-doped silicon fibers grown from the melt by the edge-defined film-fed growth technique, and reveal existence of the three critical Marangoni numbers due to thermal gradients. The homogeneity of the dopant distribution in the crystal is computed for different Marangoni numbers situated in the ranges determined by the obtained critical Marangoni numbers Ma_{c1}, Ma_{c2}, Ma_{c3}.

***Keywords*—**Boussinesq approximation, critical Marangoni number, finite element technique, fluid flow.

I. Introduction

THE demand for single or poly-silicon has increased dramatically due to the rapid expansion of the photovoltaic PV industry. Various growth techniques have been used for producing silicon wafers for a PV cell, like the Czochralski Cz, floating zone Fz and edge-defined film-fed growth EFG methods. Among these, EFG is the first non-conventional technique for crystalline silicon wafer production to enter into large-scale manufacturing in the photovoltaic industry [1], with ribbon growth of silicon meeting the actual demands of economical material consumption because it avoids silicon losses, such as during the blocking of ingots or sawing of wafers [2].

Identifying and investigating the metal impurities in silicon are fundamental tasks in semiconductor physics and device engineering. In solar cells, aluminum is usually present in the metal back contact as well as in the back surface field region. Due to a low diffusivity of interstitial aluminum in silicon, compared to the diffusivity of the transition metals, silicon is intentionally contaminated with aluminum during the growth process. If aluminum is already present as a grown-in impurity in the starting material, then it can act as an electrically-active defect with detrimental consequences to the charge carrier lifetime [3].

Molten silicon is known to be an extremely-reactive material [4], with strong thermal forcing in surface-tension-driven flows being realized during the growth process. The surface tension value and its temperature dependence are essential for describing surface-tension-driven flow (Marangoni-Bénard flow) on the free liquid surface (meniscus, i.e., the liquid bridge between the die and the crystal) [5]. It is generally accepted that thermal fluctuations are a serious drawback in growing a high-quality crystal. The existence of Marangoni convection for molten silicon has been revealed through crystal growth experiments using the Cz [6] and Fz [7] configurations. For the former, the dependence on the Marangoni-Bénard and Rayleigh-Bénard instabilities on the coefficient $d\gamma/dT$ of temperature dependence of the surface tension was confirmed. The contribution of the Marangoni effect to the instabilities and consequently to the impurity distribution in the crystal is governed by the magnitude of $d\gamma/dT$. Although a large amount of surface tension data has been reported for molten silicon [5], there is still some uncertainty concerning the absolute values and its temperature dependence, because the surface tension of molten silicon is quite sensitive to surface contamination, particularly oxygen. These reasons and the difficulty of an experimental investigation of the surface-tension-driven Marangoni-Bénard convection for small Prandtl numbers (Pr = 0.01 for silicon) have been the motivation for a numerical analysis of the dependence of the Marangoni flow and impurity distribution on the vertical temperature gradient.

This analysis is made on the aluminum-doped silicon fibers grown from the melt by EFG technique using a central capillary channel CCC shaper design (see Fig.1).

It is also assumed that, the melt level in the crucible is constant during the growth process (i.e., continuous melt replenishment) and, the radius of the fiber and the meniscus height, respectively, are constant (i.e. the effect of the pulling rate variation concerning the rod radius variation and the meniscus height variation are compensated by an adequate temperature variation).

Manuscript received September 9, 2008: Revised version received September 22, 2008. This work was supported by the North Atlantic Treaty Organisation under Grant CBP.EAP.CLG 982530.

L. Braescu is with the Computer Science Department, West University of Timisoara, Blv. V Parvan 4, Timisoara 300223, ROMANIA (corresponding author phone: +4-025-659-2221; fax: +4-025-659-2316 e-mail: lilianabraescu@ balint1.math.uvt.ro).

T. F. George is with the Chemistry & Biochemistry and Physics & Astronomy Departments, University of Missouri-St. Louis, MO 63121, USA (e-mail: tfgeorge@umsl.edu).

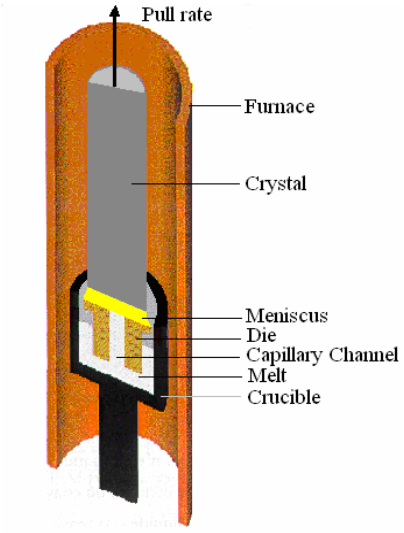

Fig.1: Schematic EFG crystal growth system.

The computations are carried out in the stationary case in a 2D axisymmetric model by the finite-element numerical technique using COMSOL Multiphysics 3.4 software [8]-[10], for 38 different values of dγ/dT situated in the maximal range [-7×10^{-4}; 0] $Nm^{-1}K^{-1}$ (i.e., for Marangoni numbers Ma between zero and 406.25), which contains all values reported in literature [5], and for three representative vertical temperature gradients in the furnace: k_{g1} = 5,000; k_{g2} = 50,000; k_{g3} = 100,000 Km^{-1} situated in the range [5,000; 100,000] Km^{-1} determined by experimental data [11]. These numerical investigations prove the existence of three critical Marangoni numbers – Ma_{c1}, Ma_{c2}, Ma_{c3} – as reported for two-dimensional containers [12]-[14]. The computed fluid flows reveal that, the best homogeneity of the dopant distribution in the crystal is obtained for lower Marangoni numbers. The length of the ranges determined by these lower Marangoni numbers increases if the vertical temperature gradient in the furnace decreases. This suggests a possible future feedback control of the Marangoni-Bénard instability which can delay the Marangoni convection [15] through a particular choice of the process parameters (for example: a small vertical temperature gradient), in order to optimize the crystal quality.

II. THE MATHEMATICAL MODEL

The Marangoni flow and impurity distribution induced by vertical temperature gradients in the furnace is analyzed in the framework of a stationary model including the incompressible Navier-Stokes equation in the Boussinesq approximation (the temperature-dependent density appears only in the gravitational force term), and the convection-conduction and conservative convection-diffusion equations [16]:

$$\begin{cases} \rho_l(\bar{\boldsymbol{u}}\cdot\nabla)\bar{\boldsymbol{u}} = \nabla\cdot\left[-p\boldsymbol{I}+\eta\left(\nabla\bar{\boldsymbol{u}}+(\nabla\bar{\boldsymbol{u}})^T\right)\right]+\beta\rho_l\bar{\boldsymbol{g}}\cdot(T-\Delta T) \\ \nabla\cdot\bar{\boldsymbol{u}} = 0 \\ \nabla\cdot(-k\nabla T+\rho_l C_p T\bar{\boldsymbol{u}}) = 0 \\ \nabla\cdot(-D\nabla c+c\bar{\boldsymbol{u}}) = 0 \end{cases} . \quad (1)$$

The axis-symmetric solutions are searched in the cylindrical-polar coordinate system (rOz) corresponding to the EFG technique having a central capillary channel shaper design (see Fig. 2).

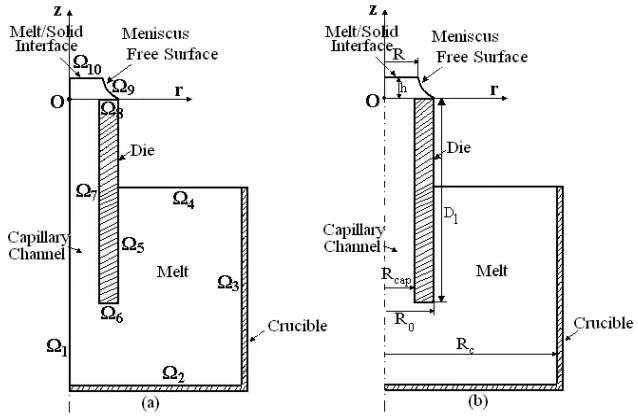

Fig. 2: Schematic EFG crystal growth system showing the domain boundaries (a) and dimensions (b) used in the numerical model.

In this system, the unknowns are: velocity vector $\bar{\boldsymbol{u}} = (u,v)$, temperature T, impurity concentration c, and pressure p. The material parameters are: ρ_l - reference melt density, β - heat expansion coefficient, η - dynamical viscosity, k - thermal conductivity, C_p - heat capacity, D - impurity diffusion, and $\bar{\boldsymbol{g}}$ - gravitational acceleration. The system (1) is considered in the two-dimensional domain whose boundary is from Ω_1 to Ω_{10}, as represented on Fig. 2(a).
The fluid density is assumed to vary with temperature as

$$\rho(r,z) = \rho_l\left[1-\beta\left(T(r,z)-\Delta T\right)\right], \quad (2)$$

and the surface tension γ in the meniscus is assumed to vary linearly with temperature as

$$\gamma(r,z) = \gamma_l + \frac{d\gamma}{dT}\left(T(r,z)-\Delta T\right) , \quad (3)$$

where $\Delta T = (T_0+T_m)/2$ is the reference temperature at the free surface, γ_l is the surface tension at the temperature ΔT, and dγ/dT is the rate of change of surface tension with the temperature. The main parameter of the Marangoni-Bénard convection is the Marangoni number

$$Ma = \left|\frac{d\gamma}{dT}\right|\cdot\frac{(T_m-T_0)\cdot h}{\eta\cdot\alpha} , \quad (4)$$

where η is the dynamic viscosity, $\alpha = k/\rho_l C_p$ is the thermal diffusivity, and h the meniscus height.
For solving the system (1), boundary conditions on Ω_1 to Ω_{10} are imposed, with the Oz-axis considered as a line of symmetry for all field variables:

- *Flow conditions*: On the melt/solid interface, the condition of outflow velocity is imposed, i.e., $\bar{\boldsymbol{u}} = \frac{\rho_l}{\rho_s}v_0\bar{\boldsymbol{k}}$, where $\bar{\boldsymbol{k}}$ represents the unit vector of the Oz-axis. On the melt level in the crucible, the inflow velocity condition is imposed (melt replenishment), $\bar{\boldsymbol{u}} = -\frac{R^2}{R_c^2-R_0^2}\cdot v_0\bar{\boldsymbol{k}}$. On the meniscus free

surface, we set up the slip/symmetry condition, $\bar{\boldsymbol{u}}\cdot\bar{\boldsymbol{n}}=0$, $\bar{\boldsymbol{t}}\cdot\left[-p\boldsymbol{I}+\eta\left(\nabla\bar{\boldsymbol{u}}+\left(\nabla\bar{\boldsymbol{u}}\right)^{T}\right)\right]\bar{\boldsymbol{n}}=0$, where $\bar{\boldsymbol{t}}$ and $\bar{\boldsymbol{n}}$ represent the tangential and normal vectors, respectively. The other boundaries are set up by the non-slip condition $\bar{\mathrm{u}}=0$.

- *Thermal conditions*: On the melt/solid interface, we set the temperature as $T = T_m$. On the free surface, we impose thermal insulation, i.e., $\bar{\boldsymbol{n}}\cdot(-k\nabla T+\rho_l C_p T\bar{\boldsymbol{u}})=0$. For the other boundaries, we have the temperature condition $T = T_0$.

- *Concentration conditions*: On the melt/solid interface, the flux condition is imposed, which expresses that impurities are rejected into the melt according to $\frac{\partial c}{\partial\bar{\boldsymbol{n}}}=-\frac{v_0}{D}(1-K_0)c$. On the melt level in the crucible, the concentration of aluminum in silicon is $c = C_0$. The other boundaries are established by insulation/symmetry, $\bar{\boldsymbol{n}}\cdot(-D\nabla c+c\bar{\boldsymbol{u}})=0$.

Imposing the above boundary conditions, on the free surface the Marangoni effect is modeled by using the weak form of the boundary application mode. Thus, on the free surface (meniscus), the boundary condition expresses that the gradient velocity field along the meniscus is balanced by the shear stress,

$$\eta\cdot\begin{bmatrix}t_r & t_z\end{bmatrix}\cdot\begin{bmatrix}2\frac{\partial u}{\partial r} & \frac{\partial u}{\partial z}+\frac{\partial v}{\partial r}\\ \frac{\partial u}{\partial z}+\frac{\partial v}{\partial r} & 2\frac{\partial v}{\partial r}\end{bmatrix}\cdot\begin{bmatrix}n_r\\ n_z\end{bmatrix}=\frac{d\gamma}{dT}\cdot\left(\frac{\partial T}{\partial r}+\frac{\partial T}{\partial z}\right), \quad (5)$$

where $\bar{\boldsymbol{t}}=(t_r,t_z)$ and $\bar{\boldsymbol{n}}=(n_r,n_z)$. The sign of the rate $d\gamma/dT$, in general, depends on the material, with downward ($d\gamma/dT<0$) or upward ($d\gamma/dT>0$) flow on the free liquid surface.

In order to investigate numerically the impurity distribution induced by the Marangoni convection and vertical temperature gradients k_g, we consider 38 values of dγ/dT situated in the range [-7×10^{-4}; 0] $\mathrm{Nm^{-1}K^{-1}}$, and three representative values of k_{g1} = 5,000, k_{g2} = 50,000 and k_{g3} = 100,000 $\mathrm{Km^{-1}}$ situated in the range [5,000; 100,000] $\mathrm{Km^{-1}}$. For every value of the vertical temperature gradient, the dependence of the fluid flow and dopant distribution on the corresponding 38 Marangoni numbers is established. The critical Marangoni numbers are found, following the computed steady or turbulent behavior of the fluid flow. In these numerical investigations, the considered diffusion coefficient of aluminum in liquid silicon is that reported recently by the new determinations of Garandet [4]. The material parameters used in the mathematical model for the considered EFG system are given in Table 1 ([4], [5], [11], [17]).

Table 1: Material parameters for silicon.

Description (units)		Value
β	heat expansion coefficient ($\mathrm{K^{-1}}$)	5.5×10^{-6}
c	impurity concentration (%)	
C_0	alloy concentration (%)	
C_p	heat capacity ($\mathrm{J\,kg^{-1}K^{-1}}$)	1040
dγ/dT	rate change of the surface tension ($\mathrm{N\,m^{-1}K^{-1}}$)	See text
D	impurity diffusion ($\mathrm{m^2s^{-1}}$)	5.8×10^{-8}
D_l	die length (m)	45×10^{-3}
g	gravitational acceleration ($\mathrm{m\,s^{-2}}$)	9.81
h	meniscus height (m)	0.5×10^{-3}
k	thermal conductivity ($\mathrm{W\,m^{-1}K^{-1}}$)	64
k_g	vertical temp. gradient ($\mathrm{K\,m^{-1}}$)	50000
K_0	partition coefficient	0.002
η	dynamical viscosity ($\mathrm{kg\,m^{-1}s^{-1}}$)	7×10^{-4}
R	crystal radius (m)	1.5×10^{-3}
R_{cap}	capillary channel radius (m)	0.5×10^{-3}
R_c	inner radius of the crucible (m)	23×10^{-3}
R_0	die radius (m)	2×10^{-3}
ρ_l	density of the melt ($\mathrm{kg\,m^{-3}}$)	2550
$\bar{\boldsymbol{u}}$	velocity vector	
v_0	pulling rate ($\mathrm{m\,s^{-1}}$)	1×10^{-7}
T	temperature (K)	
T_0	temperature at $z = h$ (K)	
T_m	melting temperature (K)	1685
ΔT	reference temperature (K)	
z	coord. in the pulling direction	

III. NUMERICAL RESULTS

The computations are made using the two-dimensional axis-symmetric hypothesis for an aluminum-doped silicon ribbon of radius $R = 1.5\times10^{-3}$ m grown with a pulling rate $v_0 = 10^{-7}$ $\mathrm{ms^{-1}}$. The boundaries presented in Fig. 2 are determined from the peculiarities of the considered EFG growth system. Thus, a crucible with inner radius $R_c = 23\times10^{-3}$ m is considered, which is continuously fed with the melt, such that the melt height in the crucible is maintained as constant at 45×10^{-3} m. In the crucible, a die with radius $R_0 = 2\times10^{-3}$ m and length is introduced, such that 2/3 of the die 45×10^{-3} m is immersed in the melt. In the die, a capillary channel of radius $R_{cap} = 0.5\times10^{-3}$ m, i.e., capillary number $Ca = 5.5\times10^{-5}$, is manufactured through which the melt rises to the top of the die, where a small meniscus of height $h = 0.5\times10^{-3}$ m is formed.

The stationary incompressible Navier-Stokes model for fluid flow, stationary heat transfer and mass transfer, along with the weak form of the boundary condition are implemented with the COMSOL Multiphysics 3.4 software, and the system (1) is solved by the finite-element numerical technique. According to the considered geometry, 17,072 triangular elements and 150,803 degrees of freedom are considered. The effect of the Marangoni forces is computed in the stationary case for the three values k_{g1} = 5,000, k_{g2} = 50,000 and k_{g3} = 100,000 $\mathrm{Km^{-1}}$ of the vertical temperature gradient in the furnace situated in the range [5,000; 100,000] $\mathrm{Km^{-1}}$ and for different Marangoni numbers Ma situated in the range [0; 406.25] (see (4)), which corresponds to those 38 considered values of the surface tension rates.

The computed fluid flows and their behaviors (downward steady flow, appearance of small turbulences, and increasing of turbulences in the meniscus) reveal the following critical

Marangoni numbers Ma_c which depend on the vertical temperature gradients:

1. For k_{g1} = 5,000 Km^{-1}, there is only one Ma_c value (Ma_{c1} = 75.4) situated in the range [0; 406.25];
2. For k_{g2} = 50,000 Km^{-1}, there are three values of Ma_c situated in the range [0; 406.25]: Ma_{c1} = 7.54, Ma_{c2} = 39.46 and Ma_{c3} = 69.64;
3. For k_{g3} = 100,000 Km^{-1}, the values of Ma_c are: Ma_{c1} = 3.65, Ma_{c2} = 19.73 and Ma_{c3} = 35.4.

These critical values are essential in the fluid flow behavior and in the dopant concentration. The connection between vertical temperature gradients and the critical Marangoni numbers can be seen on Table 2.

Table 2: The connection between vertical temperature gradients k_g and the critical Marangoni numbers Ma_c

	Ma_{c1}	Ma_{c2}	Ma_{c3}
k_{g1}=5,000 =1/10×k_{g2}	Ma_{c1} =10×Ma^*_{c1}	-	-
k^*_{g2}=50,000	Ma^*_{c1} = 7.54	Ma^*_{c2} = 39.46	Ma^*_{c3} = 69.64
k_{g3}=100,000 =2×k_{g2}	Ma_{c1} ≈1/2×Ma^*_{c1}	Ma_{c2} =1/2×Ma^*_{c2}	Ma_{c3} =1/2×Ma^*_{c3}

The computed critical Marangoni numbers (see Table 2) show that, taking as reference value k^*_{g2}=50,000, then the proportionality between vertical temperature gradients is inverse with respect of the critical Marangoni numbers. This dependence is very important for practical crystal growers, because if know critical Marangoni numbers for a fixed vertical temperature gradient, then they can compute the necessary vertical temperature gradient in the furnace such that to obtain a sufficient large range [0; Ma_{c1}] which assure a steady flow.

For the considered vertical temperature gradients k_{g1}, k_{g2} and k_{g3}, if Ma is situated in the first range [0; Ma_{c1}], then the steady downward flow ($d\gamma/dT < 0$) on the free liquid surface push the maximum of the dopant concentration C_{max} at the triple-point, as it can be seen in Figs. 3 & 4(a-c). The computed fluid velocity distribution shows that in the case for which we consider the forced flow, i.e., Ma = 0 (see Fig. 3), with a rate of 10^{-7} ms^{-1} at the solid-liquid interface (the pulling rate) if the ratio ρ_l/ρ_s is neglected, and consequently 9×10^{-7} ms^{-1} on average in the capillary channel (taking into account the surface ratio between crystal and channel), then the maximum forced velocity is 18×10^{-7} ms^{-1}. This maximum is situated in the center of the capillary channel; if the vertical temperature gradient increases, then perturbations appear.

For the case in which the surface driven flows are taken into account (Fig. 4), the Marangoni convection perturbs the forced flow: the arrows presented in Fig. 4 denote the flow of the velocity field caused by the surface tension driven flow (downward flow on the meniscus).

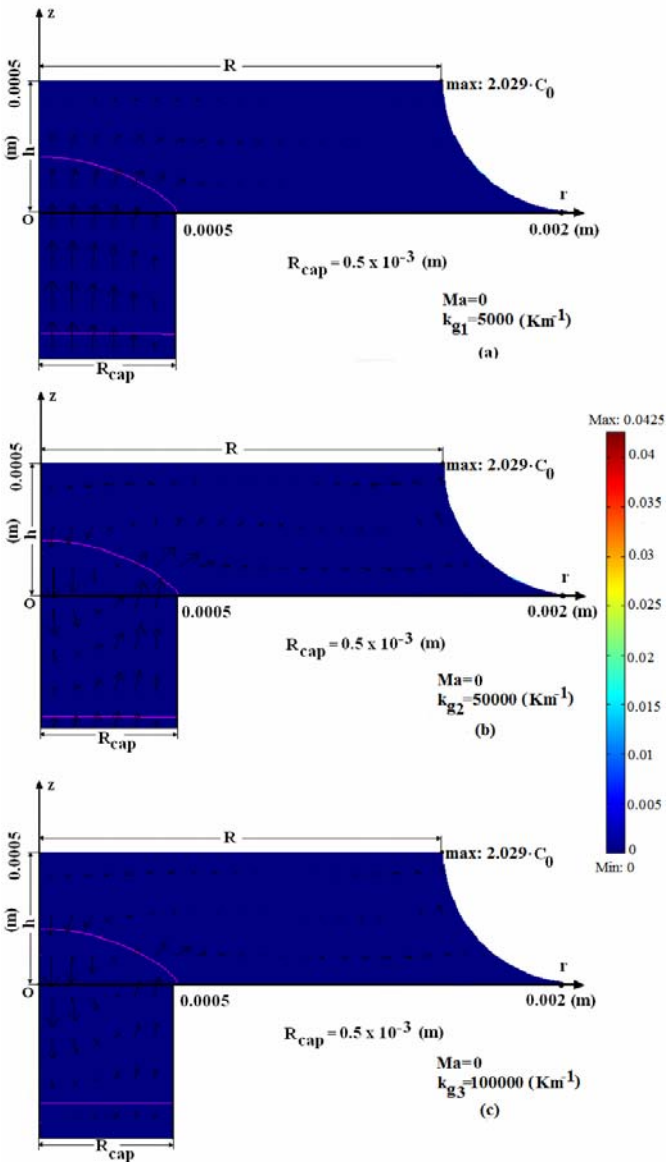

Fig. 3: Computed fluid flows and maximum values of the dopant distribution for the Marangoni number Ma = 0 in the case of k_{g1} = 5,000 Km^{-1} (a), k_{g2} = 50,000 Km^{-1} (b) and k_{g3} = 100,000 Km^{-1} (c).

The maximum velocity of the fluid flow in the meniscus is situated on the free surface, and it increases if the Marangoni number increases. This dependence and the magnitude of the maximum velocity are in agreement with the equilibrium of the viscous and Marangoni forces,

$$U \approx Ma \cdot \frac{\upsilon}{h},$$

where v is the kinematic viscosity [16].

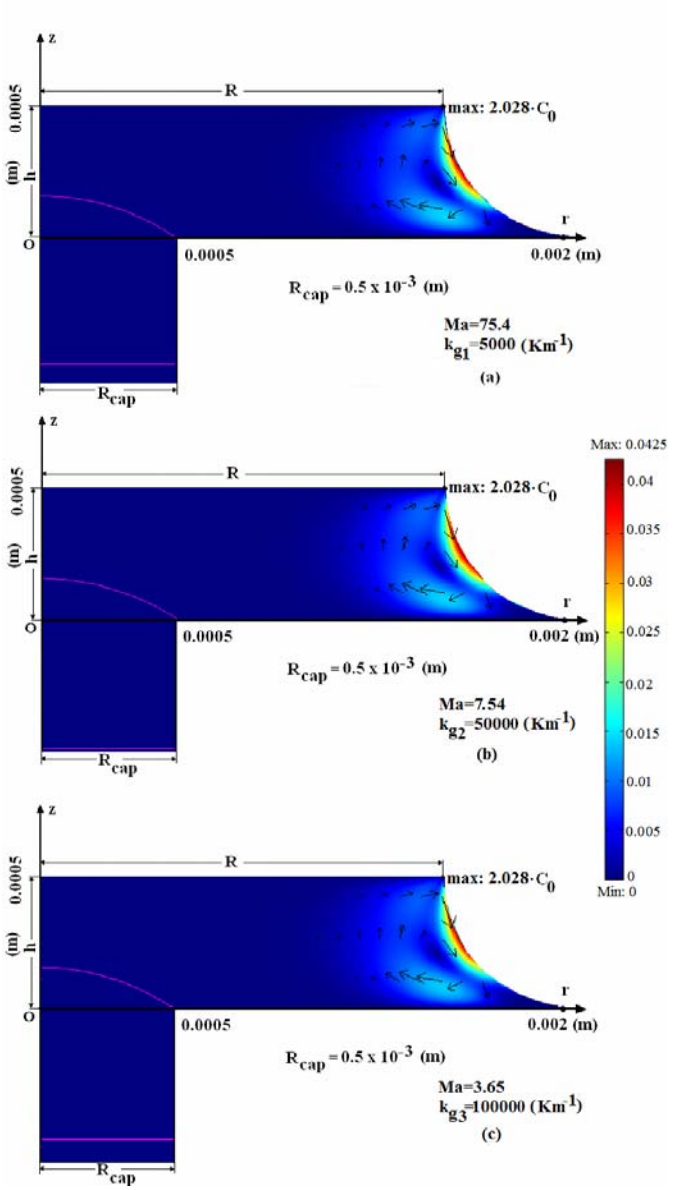

Fig. 4: Computed fluid flows and maximum values of the dopant distribution for the first critical Marangoni numbers Ma_{c1} in the case of k_{g1} = 5,000 Km^{-1} (a), k_{g2} = 50,000 Km^{-1} (b) and k_{g3} = 100,000 Km^{-1} (c).

These behaviors of the fluid flow show that if *Ma* increases in the corresponding ranges [0; Ma_{c1}], then a better mixing of the dopant distribution takes place near the free meniscus surface, and hence C_{max} decreases slowly from 2.029×C_0 (which corresponds to *Ma* = 0, Fig. 3) to 2.028×C_0 (which corresponds to *Ma*= Ma_{c1}, Fig. 4).

These investigations prove that, for any vertical temperature gradients k_{g1}, k_{g2} and k_{g3}, the fluids flow and dopant distributions are similar for *Ma* in the range [0; Ma_{c1}]. The most important point is the length of the interval [0; Ma_{c1}], which depends on the size of the vertical temperature gradient. For practical crystal growers, this information offers the possibility to change the configuration of the equipment and process parameters (vertical temperature gradient) for optimization of the crystal quality.

Concerning of the second (Ma_{c2}) and third (Ma_{c3}) critical Marangoni numbers, computations show that if *Ma* increases in the ranges (Ma_{c1}; Ma_{c2}], (Ma_{c2}; Ma_{c3}] and (Ma_{c3}; 406.25] for k_{g2} and k_{g3}, or if *Ma* increases in the range (Ma_{c1}; 406.25] for k_{g1}, the velocity of the fluid flow in the meniscus increases, and turbulences in the fluid flow take place. More precisely, if *Ma* increases in the range (Ma_{c1}; Ma_{c2}] for k_{g2} and k_{g3} (or if *Ma* increases in the range (Ma_{c1}; 406.25] for k_{g1}) then very small turbulences in the fluid flow lead to an increase of C_{max}, which is located at the triple-point. If *Ma* increases in the range (Ma_{c2}; Ma_{c3}], then turbulences in the fluid increase, and C_{max} is pushed inside at the level of the melt/crystal interface, at a distance on the same order as the meniscus height from the external crystal surface (see Fig. 5).

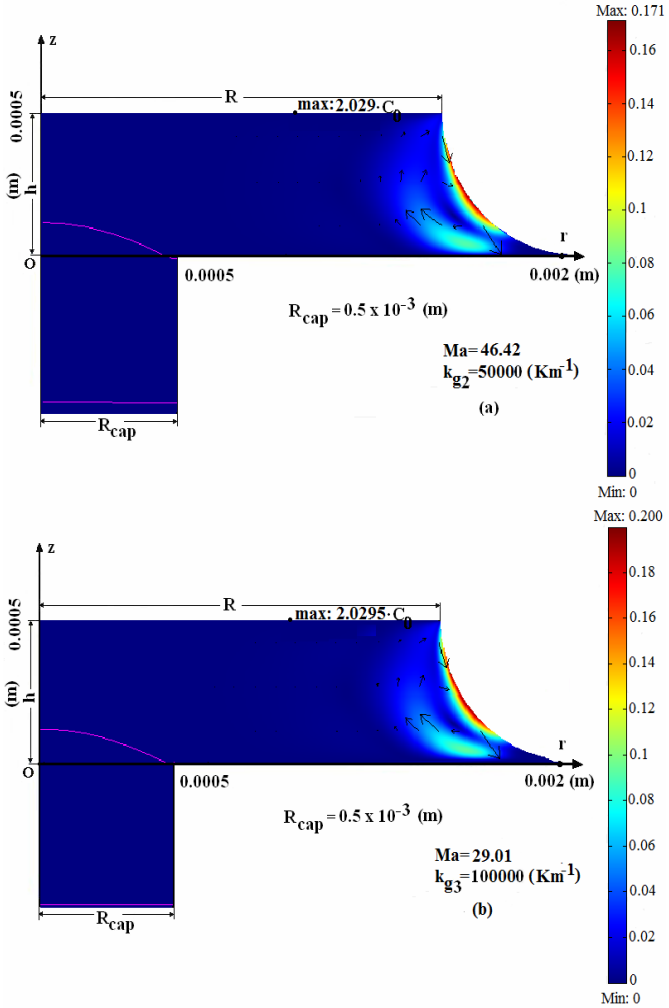

Fig. 5: Computed fluid flows and maximum values of the dopant distribution for the Marangoni numbers in the range (Ma_{c2}; Ma_{c3}]: *Ma* = 46.42 for k_{g2} = 50,000 Km^{-1} (a) and *Ma* = 29.01 for k_{g3} = 100,000 Km^{-1} (b).

If *Ma* increases in the range (Ma_{c3}; 406.25], then higher turbulences move C_{max} at the triple-point which increases considerably.

Investigations show that for smaller vertical temperature gradients we obtain a wide range [0; Ma_{c1}] of values of the surface tension temperature coefficients which

assures the best homogeneity of the crystal. Indeed, non-homogeneity of the crystal is given by the reduced radial segregation

$$\Delta C = \frac{C_{max} - C_{ax}}{C_{ax}},$$

where $C_{max} = K_0 \cdot c_{max}(r, h) = K_0 \cdot c_{max}(r; 0.5\times10^{-3})$ represents the maximum concentration in the crystal, and $C_{ax} = K_0 \cdot c(0,h) = K_0 \cdot c(0; 0.5\times10^{-3})$ represents the concentration on the axis of the crystal. For the representative vertical temperature gradient $k_{g2} = 50{,}000$ Km^{-1}, the effect of the Marangoni forces on the radial segregation can be seen on the Fig. 6 (a-d) in which the radial segregations are presented as function of the Marangoni numbers situated in the intervals [0; Ma^*_{c1}], (Ma^*_{c1}; Ma^*_{c2}], (Ma^*_{c2}; Ma^*_{c3}] and (Ma^*_{c3}; 406.25], defined by the critical values.

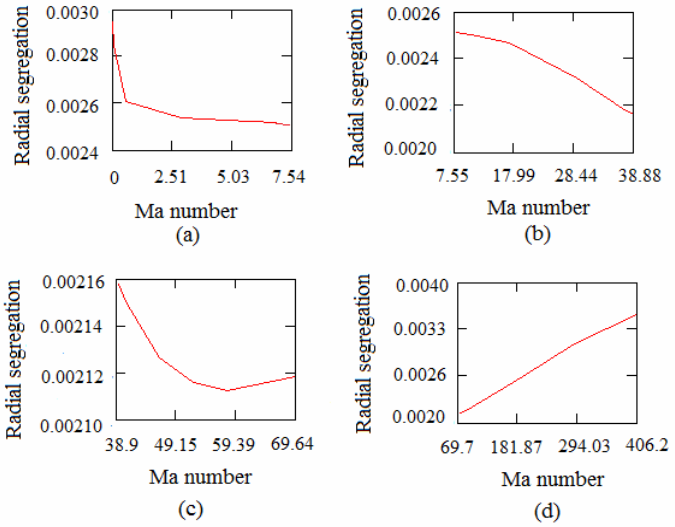

Fig. 6: Computed radial segregations for the Marangoni numbers situated in the ranges [0; Ma^*_{c1}] (a), (Ma^*_{c1}; Ma^*_{c2}] (b), (Ma^*_{c2}; Ma^*_{c3}] (c) and (Ma^*_{c3};406.25] (d).

These plots show that the radial segregation ΔC does the following:

(i) decreases from 2.9×10^{-3} to 2.5×10^{-3} for Ma in [0; Ma^*_{c1}];
(ii) decreases from 2.5×10^{-3} to 2.1×10^{-3} for Ma in (Ma^*_{c1}; Ma^*_{c2}];
(iii) is around 2.1×10^{-3} for Ma in (Ma^*_{c2}; Ma^*_{c3}], showing a slight increase; and (iv) for Ma larger than Ma^*_{c3}, ΔC increases considerably.

IV. Conclusion

The dependences of the Marangoni flow and impurity distribution on the vertical temperature gradient in aluminum-doped silicon fibers, grown from the melt by the EFG method, are determined numerically by the finite-element technique in the framework of a stationary model including incompressible fluid flow in the Boussinesq approximation, heat and mass transfer, and the Marangoni effect. The computed fluid flows and their behaviors (downward steady flow, appearance of small turbulences, and increasing of turbulences in the meniscus) reveal the existence of three critical Marangoni numbers, Ma_{c1}, Ma_{c2} and Ma_{c3}, which depend on the vertical temperature gradients. The wide range [0; Ma_{c1}] over which the downward steady flow induce the best homogeneity of the dopant distribution is obtained for the smaller considered vertical temperature gradient. This suggests to practical crystal growers that a possible feedback control for delaying the Marangoni convection can be obtained by decreasing vertical temperature gradient in the furnace. This control can be realized by other choices of the process parameters, e.g., by applying magnetic fields [18], which suggest further developments near the future.

A conclusion section is not required. Although a conclusion may review the main points of the paper, do not replicate the abstract as the conclusion. A conclusion might elaborate on the importance of the work or suggest applications and extensions.

Acknowledgment

L. Braescu, and T. F. George thank to the North Atlantic Treaty Organisation (Grant CBP.EAP.CLG 982530).

References

[1] B. Yang, L. L. Zheng, B. Mackintosh, D. Yates, and J. Kalejs, "Meniscus dynamics and melt solidification in the EFG silicon tube growth process," *Journal of Crystal Growth*, vol. 293, August 2006, pp. 509-516.

[2] H. Kasjanow, A. Nikanorov, B. Nacke, H. Behnken, D. Franke, and A. Seidl, "3D coupled electromagnetic and thermal modeling of EFG silicon tube growth," *Journal of Crystal Growth*, vol. 303, May 2007, pp. 175-179.

[3] P. Rosenits, T. Roth, S. Glunz, and S. Beljakowa, "Determining the defect parameters of the deep aluminum-related defect center silicon," *Applied Physics Letters*, vol. 91, September 2007, pp. 122109:1-122109:3.

[4] J. P. Garandet, "New determinations of diffusion coefficients for various dopants in liquid silicon," *International Journal of Thermophysics*, vol. 28/4, August 2007, pp. 1285-1303.

[5] M. Przyborowski, T. Hibiya, M. Eguchi, and I. Egry, "Surface tension measurement of molten silicon by the oscillating drop method using electromagnetic levitation," *Journal of Crystal Growth*, vol.151, May 1995, pp. 60-65.

[6] K.-W. Yi, K. Kakimoto, M. Eguchi, M. Watanabe, T. Shyo, and T. Hibiya, "Spoke patterns on molten silicon in Czochralski system," *Journal of Crystal Growth*, vol. 144, November 1994, pp. 20-28.

[7] S. Nakamura, T. Hibiya, K. Kakimoto, N. Imaishi, S. Nishizawa, A. Hirata, K. Mukai, S. Yoda, and T. S. Morita, "Temperature fluctuations of the Marangoni flow in a liquid bridge of molten silicon under microgravity on board the TR-IA-4 rocket," *Journal of Crystal Growth*, vol.186, March 1998, pp. 85-94.

[8] L. Braescu, T. F. George, and St. Balint, "Mass transfer analysis in the case of the EFG method", in *Proceedings of the European Computing Conference*, vol. 2, edited by N. Mastorakis, V. Mladenov, V. Kostargyri, Norwell, Massachusetts: Springer, 2009, pp. 1345-1356

[9] L. Braescu, and T. F. George, "Arbitrary Lagrangian-Eulerian method for coupled Navier-Stokes and convection-diffusion equations with moving boundaries," in in *Proc. 12th WSEAS International Conference on Applied Mathematics – Math'07*, Cairo, 2007, pp. 33-36.

[10] N. M. Arifin, and H. Rosali, "On competition between modes of the onset of Marangoni with free-slip bottom under magnetic field," in *Proc. 12th WSEAS International Conference on Applied Mathematics – Math'07*, Cairo, 2007, pp. 87-91.

[11] O. Bunoiu, I. Nicoara, J. L. Santailler and T. Duffar, "Fluid flow and solute segregation in EFG crystal growth process," *Journal of Crystal Growth*, Vol. 275, vol 275, February 2005, pp. e799-e805.

[12] T. Boeck, and A. Thess, "Inertial Benard-Marangoni convection," *Journal of Fluid Mechanics,* vol. 350, November 1997, pp. 149-175.

[13] K. A. Cliffe, and S. J. Tavener, "Marangoni-Benard convection with a deformable free surface," *Journal of Computational Physics*, vol. 145, September 1998, pp. 193-227.

[14] T. Boeck, "Bénard-Marangoni convection at large Marangoni numbers: results of numerical simulations," *Advances in Space Research*, vol. 36, January 2005, pp. 4-10.

[15] N. M. Arifin, R. M. Nazar, and N. Senu, Feedback control on the Marangoni-Bénard instability in a fluid layer with a free-slip bottom, *Journal of the Physical Society of Japan*, vol.76, January 2007, pp. 014401:1-014401:4.

[16] L. Braescu, and T. Duffar, "Effect of buoyancy and Marangoni forces on the dopant distribution in a single crystal fiber grown from the melt by edge-defined film-fed growth (EFG) method," *Journal of Crystal Growth*, vol. 310, January 2008, pp. 484-489.

[17] J. P. Kalejs, "Modeling contributions in commercialization of silicon ribbon growth from the melt," *Journal of Crystal Growth*, vol. 230, August 2001, pp. 10-21.

[18] P. Dold, A. Croll, and K. W. Benz, "Floating-zone growth of silicon in magnetic fields. I. Weak static axial fields," *Journal of Crystal Growth*, vol.183, February 1998, pp. 545-553.

Liliana Braescu was born in ROMANIA, in 1967. She received her PhD in mathematics from West University of Timisoara, Romania, in 2002.

She has held positions in secondary and high schools, as well in undergraduate and postgraduate level: Mathematics teacher at the Secondary School "Avram Iancu", Timisoara, 1991-93; Mathematics teacher at the High School "Colegiul National Banatean" Timisoara 1993-99; Assistant Professor in Department of Mathematics, Technical University of Timisoara, 1999-2003; Lecturer in Department of Mathematics, Technical University of Timisoara, 2003-04; Senior Lecturer in the Faculty of Mathematics and Computer Science, West University of Timisoara, 2004-06; Associate Professor in the Faculty of Mathematics and Computer Science, West University of Timisoara, 2006-present. Her research has led to 26 papers published in refereed journals, 6 chapters in books (Springer, Cambridge Scientific Publishers, Nova Science Publishers, Wiley & Sons), 1 textbook, 58 communications to scientific meetings (26 published in proceedings), 9 course materials. The representative publications are the following: (1) T. F. George, L. Braescu, A. M. Balint, L. Nánai and S. Balint, *Microcomputer Modeling of Growth Processes of Single-Crystal Sheets and Fibers*. Hauppauge, New York: Nova Science Publishers, 2007, 199 pages; (2) S. Balint, L. Braescu, E. Kaslik, *Regions of Attraction and Applications to Control Theory,* edited by S. Sivasundaram, Cambridge Scientific Publishers, 2008, 206 pages; (3) L. Braescu, "Shape of menisci in terrestrial dewetted Bridgman growth", *Journal of Colloid and Interface Science*, vol. 319, pp. 309-315 (2008). Her research interests include control theory, ordinary and partial differential equations, stability and domains of attractions with applicability in modelling of the crystal growth processes, blood coagulation, and dental endosteal implantation.

Associate Professor Braescu has been a member of the following professional societes and organizations: The International Society of Optics and Photonics (SPIE), European Materials Research Society (E-MRS), World Scientific and Engineering Academy and Society (WSEAS), Sigma Xi, Ad Astra Association – Romanian Scientific Community, Romanian Mathematical Society.

Thomas F. George was born in Philadelphia, USA, in 1947. He received his B.A. degree (*Phi Beta Kappa*) in chemistry (with honors) and mathematics (with honors) from, Gettysburg College in Pennsylvania, in 1967. He then received his M.S. degree in chemistry from Yale University 1968 and his Ph.D. degree in chemistry from Yale University in 1970.

He has held the following position in chronological order: Research Associate, Massachusetts Institute of Technology, 1970-71; Postdoctoral Appointee, University of California at Berkeley, 1971-72; Assistant Professor of Chemistry, University of Rochester (New York), 1972-74; Associate Professor of Chemistry, University of Rochester, 1974-77; Professor of Chemistry, University of Rochester, 1977-85; Dean of Natural Sciences and Mathematics / Professor of Chemistry and Physics, State University of New York at Buffalo, 1985-91; Adjunct Professor of Chemistry and Physics, State University of New York at Buffalo, 1991-93; Provost and Academic Vice President / Professor of Chemistry and Physics, Washington State University, 1991-96; Adjunct Research Professor of Physics, Korea University (Seoul, Korea), 1994-99; Chancellor / Professor of Chemistry and Physics, University of Wisconsin–Stevens Point, 1996-2003; Visiting Professor of Physics, Korea University (Seoul, Korea), 1999-2006; and Chancellor / Professor of Chemistry and Physics, University of Missouri–St. Louis, 2003-present. His research has led to 685 articles/chapters; 5 textbooks on various aspects of quantum/classical mechanics and chemical/materials/optical/nano-physics; 15 edited books/volumes; and 205 conference abstracts. Three recent books are: (1) T. F. George, L. Braescu, A. M. Balint, L. Nánai and S. Balint, *Microcomputer Modeling of Growth Processes of Single-Crystal Sheets and Fibers*. Hauppauge, New York: Nova Science Publishers, 2007, 199 pages; (2) L. Tilstra, S. A. Broughton, R. S. Tanke, D. Jelski, V. A. French, G. P. Zhang, A. K. Popov, A. B. Western and T. F. George, *The Science of Nanotechnology: An Introductory Text*. Hauppauge, New York: Nova Science Publishers, 2008, 185 pages; and (3) G. A. Mansoori, T. F. George, L. Assoufid and G. P. Zhang, Editors, *Molecular Building Blocks for Nanotechnology: From Diamondoids to Nanoscale Materials and Applications*. New York: Springer, 2007, 440 pages. His research interests are in the theory of laser-induced chemical physics, nonlinear optics, molecular collision dynamics, chemical reactions, energy transfer, molecular clusters/nanostructures, fractals, surface and solid-state chemistry/physics, high-temperature superconductivity and polymers.

Professor George has been a member of the following professional societies and organizations: American Chemical Society, 1968-present; American Physical Society, 1968-present; Sigma Xi, 1970-present; Royal Society of Chemistry (Great Britain), 1975-present; New York Academy of Sciences, 1979-present; Society of Photo-Optical Instrumentation Engineers, 1979-present; Council of Colleges of Arts and Sciences, 1985-91; Buffalo Society of Natural Sciences, 1986-present; European Physical Society, 1986-2003; American Association for the Advancement of Science, 1989-present; Materials Research Society, 1992-present; Northwest Scientific Association, 1992-96; Northwest Academic Forum, Western Interstate Commission for Higher Education, 1992-96; and American Society for Laser Medicine and Surgery, 2003. His honors and awards include the following: Camille and Henry Dreyfus Foundation Teacher-Scholar, 1975-85; Alfred P. Sloan Foundation Research Fellow, 1976-80; Marlow Medal and Prize, Royal Society of Chemistry (Great Britain), 1979; New York Academy of Sciences Fellow, 1981; John Simon Guggenheim Memorial Foundation Fellow, 1983-84; American Physical Society Fellow, 1984; Society of Photo-Optical Instrumentation Engineers Fellow, 1994; American Association for the Advancement of Science Fellow, 1994; Outstanding Contributions to Chemistry Award, Central Wisconsin Section, American Chemical Society, 2002; Korean Academy of Science and Technology (foreign member), 2004; and honorary doctorate in physics (*honoris causa*), University of Szeged, Hungary, 2008.